Research Article

Zhan Jia, Lixia Guo, Ling Zhong*, and Yuqing Yang

Experimental study on the influence of aggregate morphology on concrete interfacial properties

https://doi.org/10.1515/secm-2024-0025
received March 29, 2024; accepted June 07, 2024

Abstract: Aggregate is the basic component of concrete, and its shape and surface properties largely determine the mechanical properties and durability of concrete. In order to further study the mesoscopic influence of aggregate shape on concrete interfacial phase, this study focuses on two aggregate shapes, circular and polygonal, and the elastic modulus and hardness of interfacial phase of specimens with different aggregate shapes were obtained by nano-indentation technology, and the mesoscopic component partition was quantified. Based on Gaussian statistical theory, the distribution model of nanomechanical properties of each phase was established, and the influence of aggregate shape on mechanical properties was studied by SEM test. The results show that (1) The width of the interfacial zone of natural rounded aggregate (~50 μm) is slightly smaller than that of polygonal aggregate (~60 μm), and the modulus of elasticity and hardness of the interfacial zone corresponding to the rounded aggregate (*e.g.*, interfacial transition zone (E,H) ~ (23.65 GPa, 0.9 GPa)) are larger than that of the interfacial zone of polygonal aggregate (interfacial transition zone (E,H) ~ (21.66 GPa, 0.73 GPa)), indicating that the micromechanical properties of the interfacial zone of the circular aggregate are better than those of the polygonal aggregate; (2) The hydration products in the transition zone of the interface of different shapes of aggregates are almost the same, indicating that the influence of the shape of aggregates on the performance of concrete is mainly due to its own geometric characteristics. Based on the findings of the study, the direction of future research can focus on modeling with further refinement of the influence of aggregate shape parameters, such as shape factor and surface roughness, on the performance of concrete, so as to facilitate more accurate prediction and regulation of the performance of concrete. This study provides theoretical references for the design of aggregate proportioning and the simulation technology of fine data values in actual projects, and also provides theoretical basis and technical support for the standardization and performance evaluation of concrete materials.

Keywords: aggregate shape, Gaussian mixture model, nano indentation technology, SEM test, nanomechanical properties

1 Introduction

At the meso-level, concrete is generally considered to be a heterogeneous composite composed of coarse aggregate, cement mortar, and the interface transition zone (ITZ) between the two, and the properties of each of its phase materials affect the mechanical properties of concrete. Studies have shown that coarse aggregate has a great influence on the various mechanical properties of concrete [1]. The shape of the coarse aggregate will cause stress concentration in concrete, resulting in cracks on the macroscopic surface of concrete and changes in meso-structure [2]. The transition zone between coarse aggregate and interface of concrete composites tends to be prone to larger microcracks, while the water absorption of concrete is closely related to the structure of the cement matrix and the ITZ area. It was found by Golewski [3] that the composition and modification of the binder will make the composite structure more homogenized, which can effectively inhibit the initial internal damage of concrete, and it was found that the addition of a moderate amount of coal fly ash (FCA) can effectively improve the durability of the concrete structure under water immersion conditions [4], while an increase in the content of FCA leads to a significant change in the

* **Corresponding author: Ling Zhong,** School of Water Conservancy, North China University of Water Resources and Electric Power, Zhengzhou, 450046, China; Henan Key Laboratory of Water Environment Simulation and Treatment, Zhengzhou, 450002, China, e-mail: zhongling@ncwu.edu.cn
Zhan Jia: School of Water Conservancy, North China University of Water Resources and Electric Power, Zhengzhou, 450046, China, e-mail: 771916800@qq.com
Lixia Guo: School of Water Conservancy, North China University of Water Resources and Electric Power, Zhengzhou, 450046, China; Henan Key Laboratory of Water Environment Simulation and Treatment, Zhengzhou, 450002, China, e-mail: guolx@126.com
Yuqing Yang: School of Water Conservancy, North China University of Water Resources and Electric Power, Zhengzhou, 450046, China, e-mail: 1942077941@qq.com

process of fracture of the concrete structure [5]. Concrete coarse aggregate is usually natural aggregate and artificial aggregate. Natural aggregate due to natural weathering and erosion has usually smooth surface, with round or oval, while artificial aggregate is machined into polygons. It is generally believed that with the increase in coarse aggregate content, the more coarse aggregate has a shape close to sphere or regular polyhedron, the more obvious and favorable the growth of compressive strength and elastic modulus of the concrete is [6]. The more irregular and rough the shape and surface texture of the coarse aggregate, the greater the porosity, the better the permeability, and the worse the durability of the concrete in the ITZ [7–10]. In the process of concrete mix ratio design or engineering design of hydraulic engineering, how to reasonably select coarse aggregate is an engineering problem and a scientific problem, and studying the influence of aggregate shape on concrete has become an important work.

In the past, researchers mainly used macroscopic technical means to discuss the influence of aggregate on concrete. Shi *et al.* [11] showed that the type and shape of aggregate had an impact on the distribution of elements inside the concrete, and the thickness of the ITZ was also different, and the higher the concentration of $Ca(OH)_2$ in the ITZ, the greater the thickness and the worse the mechanical properties. Yehia *et al.* [12] used two kinds of natural aggregate and two kinds of lightweight recycled aggregate for concrete mixing, studied the influence of aggregate type and shape on the compressive strength of concrete at different ages, and adopted the statistical method of hypothesis testing, and the test results showed that the type and shape of aggregate had significant influence on the compressive strength and elastic modulus. Wu *et al.* [13] conducted a 28-days compressive test, and the test results showed that under the same water-binder ratio, the aggregate type had no obvious influence on the ordinary concrete, but had a significant influence on the compressive strength of high-strength concrete.

The nanoindentation technology provides a new channel for exploring the connection between the micromechanical properties and the macroscopic mechanical properties of concrete. Velez *et al.* [14] and Ulm *et al.* [15,16] calculated and analyzed the indentation elastic modulus and hardness of each phase component in the microstructure of concrete materials by using mathematical statistics method through nanoindentation test. Wu [17] used nanoindentation test to test the change in elastic modulus of each phase component of concrete under freeze-thaw conditions. Zhou *et al.* [18] studied the microstructure and formation mechanism of cement-based materials by using nanoindentation testing technology, and the results showed that the differences of hydration products in cement slurry were caused by the composition of cementing materials, water-binder ratio, and hydration age. Smerdova *et al.* [19] analyzed the indentation cycling behavior of polymers and solved the problem of the time dependence of the parameters involved by evaluating the instantaneous elastic modulus of the polymer, the dissipative behavior, and the evolution of the ratchet. However, there are relatively few studies on the effect of aggregate shape on the microscopic damage of concrete, and its macroscopic mechanical properties are determined by the internal fine structure, and the macroscopic failure behavior is also due to the accumulation and development of its damage at the fine level [20,21]. Therefore, this work adopts the nanoindentation test technique to carry out microscopic tests on specimens with different shapes of aggregates, and uses the Gaussian mixture model deconvolution method to compute the nanoindentation test data and analyze the micromechanical characteristics of the aggregates; SEM test material phase analysis is carried out to study the effects of two different shapes of natural aggregates, circular and polygonal, on the interfacial phases of concrete.

2 Test method principle

2.1 Principle of nanoindentation test

The working principle of the nanoindentation test is to measure the magnitude of the force of the indenter during indentation and the displacement of the indenter into the surface of the sample, and then record these data in real time, so as to obtain the load–displacement curves ($P-h$ curves) of the tested material, and then by analyzing the mechanical response relationship contained in the $P-h$ curve data, establish the corresponding mechanical model to identify and analyze a variety of mechanical parameters of the tested material [22].

The hardness H of the material measured can be obtained from the ratio of the maximum load to the projected contact area as in Equation (1) below:

$$H = \frac{F_{\max}}{A_c}, \tag{1}$$

where is the maximum load and A_c is the projected contact area. For the indenter with specific geometry, there is a functional relationship between the projected contact area and the contact depth h_c. For the Berkovich indenter used in this test, the area function is shown in Equation (2).

$$A_c = 24.56 \times h_c^2. \quad (2)$$

Meanwhile the contact depth h_c can be obtained from the load-displacement result, which is calculated as shown in Equation (3).

$$h_c = h - \varepsilon \frac{F}{S}, \quad (3)$$

where ε is a constant related to the indenter geometry, and for the Berkovich indenter used in this test, ε is 0.75 and S is the contact stiffness.

The modulus of elasticity of the measured material can be calculated using Equation (4).

$$E = (1 - \upsilon^2)\left[\frac{1}{E_r} - \frac{(1 - \upsilon_i^2)}{E_i}\right]^{-1}, \quad (4)$$

where υ denotes the Poisson's ratio of the measured material, for cement-based materials, υ takes the value of 0.2; E_i and υ_i denote the elastic modulus and Poisson's ratio of the indenter, for the diamond indenter, E_i takes the value of 1,114 GPa, υ_i takes the value of 0.07; and E_r is the indentation modulus, which is calculated based on the theory of elastic contact, and is shown in Equation (5).

$$E_r = \frac{\sqrt{\pi}}{2\beta\sqrt{A_c}} S. \quad (5)$$

2.2 Deconvolution methods for Gaussian mixture models (GMM)

The deconvolution method of GMM was used to process and analyze the data of nano test. Based on the method of statistical mechanics, the mechanical property parameters $x_i = (E, H)$ of each phase of the specimen should conform to normal distribution or Gaussian distribution [23], and is shown in Equation (6).

$$f_i(x_i, \mu_j, \sigma_j^2) = \frac{1}{\sigma_j\sqrt{2\pi}} \exp\left(-\frac{(x_i - \mu_j)^2}{2\sigma_j^2}\right), \quad (6)$$

where, x_i is the indentation modulus of elasticity or hardness; μ_j is the sample mean, $\mu_j = \frac{1}{N_j}\sum_{i=1}^{N_j} x_i$; σ_j^2 is the sample variance, $\sigma_j^2 = \frac{1}{N_j - 1}\sum_{i=1}^{N_j}(x_i - \mu_j)^2$; and N_j is the number of all test points corresponding to j-th in the sample data.

3 Test

3.1 Preparation of test materials and specimens

3.1.1 Test materials

The test materials are P · O 42.5 ordinary Portland cement and grade I fly ash from Henan Yulian Power Plant, the gravel material in the coarse aggregate is natural pebbles from a river bed in Xuchang, after artificial screening, the particle size is 5–31.5 mm, the bulk density is 1669.3 kg/m^3, and the aggregate can be cut to form polygonal aggregate. Because the microscopic test has high requirements on the test surface, and in order to compare the influence of aggregate on the interface area, a single aggregate paste sample was prepared for the test. The test is shown in Table 1.

3.1.2 Specimen preparation

In order to facilitate the observation of the interface between the different aggregates and the net slurry, and to reduce the high degree of damage to the specimens during the polishing process, the regular rounded gravel and irregular polygonal crushed stone aggregates were cut into flatter planes in advance, as shown in Figure 1. This treatment reduces the discrete nature of the data and thus reduces the interference of the specimens themselves in the test results [24]. Adopting the method of specimen preparation from literature [25] (1) before the test, the pebbles were cut and polished, and their mass was controlled to be 10.5 g, and the polished aggregate was cleaned, saturated, and face-dried; (2) then the saturated and face-dried aggregate was mixed with the required cement and fly ash for 1 min; (3) 50% of the required water was added, and the

Table 1: Test mix ratio

Classification	Water-binder ratio	Cement (kg/m^3)	Fly ash (kg/m^3)	Water (kg/m^3)	Aggregate shape
A	0.4	70	20	36	Circle
B	0.4	70	20	36	Polygon

Figure 1: Aggregate with the flat surface cut out.

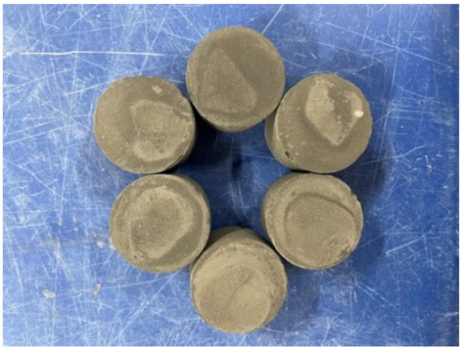

Figure 2: Sample after demolding.

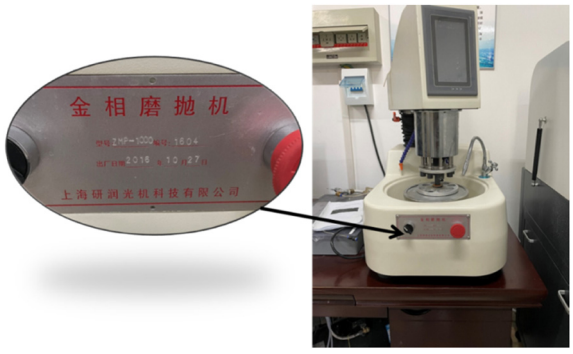

Figure 3: Metallographic polishing machine.

mixture was stirred for 1 min; (4) finally, the remaining water was added to the mixture and the stirred for 2 min, the stirred mixture was loaded into a cylindrical mold with the size of ∅ 30 mm × 20 mm (one aggregate was put into each mold), placed on the shaking table for 2 min, and placed in a room at 20 ± 5°C for 24 h after demolding. The demolded specimens are shown in Figure 2, and finally the specimens were placed in the standard curing room for the standard curing.

7d age specimens into the anhydrous alcohol soaked for 2d, and then sequentially in the 400–5000 mesh sandpaper on the coarse grinding (coarse grinding method to follow the "8" method). In order to ensure that the top and bottom sides of the specimen are parallel to each other and to make the contour of the aggregate in the specimen more visible, the specimen is polished and fine ground on the ZMP-1000 metallographic grinder (Figure 3). During the grinding process, the faucet was turned on at the same time and the specimen was rinsed with running water. The abrasive paper was selected in order of 1,000 mesh, 1,500 mesh and 2,000 mesh for grinding. Then, the specimens were further finely ground and repeatedly polished using 1 μm and 0.5 μm diamond polishing solutions until a mirror-like smooth surface was obtained, as shown in Figure 4. Finally, the polished specimens were ultrasonically cleaned with the ultrasonic cleaner in Figure 5, and the cleaning time was set to 4 min, in order to remove the particles and powders that might be attached. It is also necessary to ensure that the surface roughness of the polished specimen is within 100 nm.

3.2 Nanoindentation test

The number of indentation points has an effect on the analysis of Nanoindentation test data. When the number of indentation points is greater than 225, the test data are more stable [26]. The number of indentation points in the

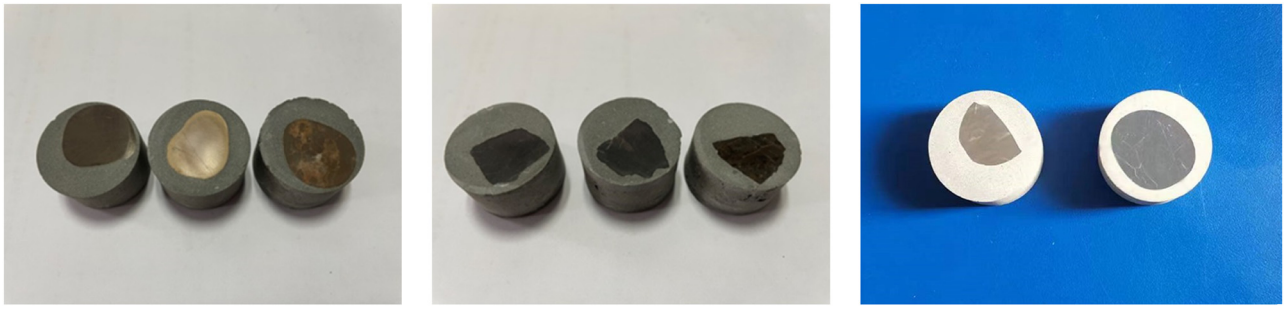

Figure 4: Sample after polishing.

Figure 5: Ultrasonic cleaning machine.

test is 30 × 10 rectangular lattice (along the vertical aggregate direction, the distance between the two points is 10 μm; along the direction of parallel aggregate, the distance between the two points is 30 μm), and the lattice area is selected at the junction of aggregate and paste, as shown in Figure 6. The test was completed on the Nano Indenter G200 nanoindentation instrument to obtain the elastic modulus E and hardness H of each point. The maximum load of the test is 500 mN, the single point loading time is 25 s, the load holding time is 10 s, and the cycle is five times to eliminate the micro creep and thermal drift effects [27].

3.3 Scanning electron microscope (SEM) test

Hitachi SU8000 series ultra-high resolution field emission scanning electron microscope SU8020 combined with high-performance HORIBA EX-350 was used to characterize the phase of the ITZ of different aggregate shapes, and the influence of aggregate shapes on the hydration products in the clean pulp was analyzed. The specimen after the nanoindentation test is cut into a sample containing aggregate and interface, dried in a drying oven, fixed on the conductive glue on the sample base, and coated with gold coating for testing.

4 Results and mechanism analysis

4.1 Influence of aggregate morphology on interface parameters

Due to the high precision requirements of the microscopic test, the test environment and other factors lead to invalid data in the results, the number of invalid points in the two groups of nanoindentation data is 11 and 17, respectively, accounting for 3.6 and 5.6% of the total number of indentation points, and the data are reasonable and reliable. After the anomalous points were eliminated in the process of data collation, the average value of the data adjacent to the right and left sides of the anomalous points was taken to fill in, and the change in the modulus of elasticity and hardness of different aggregate shapes from the distance of the surface of the aggregate were plotted and clouded in Figures 7 and 8, respectively.

It can be seen from (a) and (c) in Figures 7 and 8 that the elastic modulus and hardness decrease first and then tend to be uniform and stable as the distance from the surface of the circular aggregate increases. The elastic modulus and hardness decrease sharply when the distance from the surface of the circular aggregate is about 0–15 μm. In the range of 15–50 μm from circular aggregate, the decreasing trend of elastic modulus and hardness slows down. The micromechanical parameters tend to be stable in the range of 50–180 μm. According to (b) and (d) in Figures 3 and 4, as the distance from the surface of the polygonal aggregate increases, the modulus of elasticity

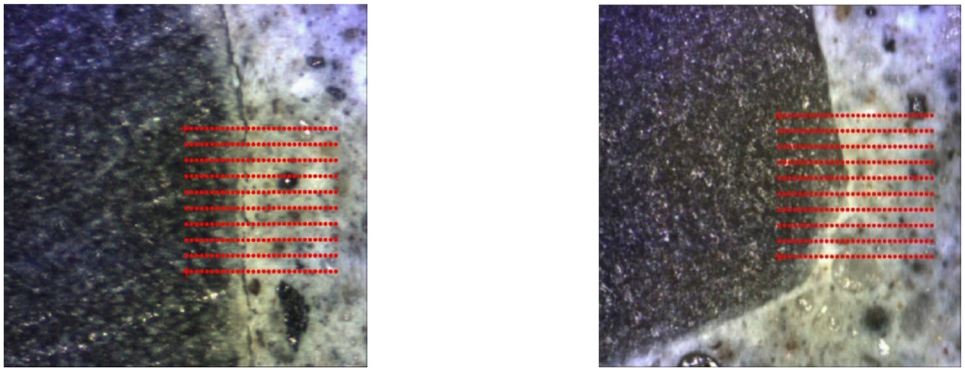

Figure 6: Schematic diagram of nanoindentation experiment.

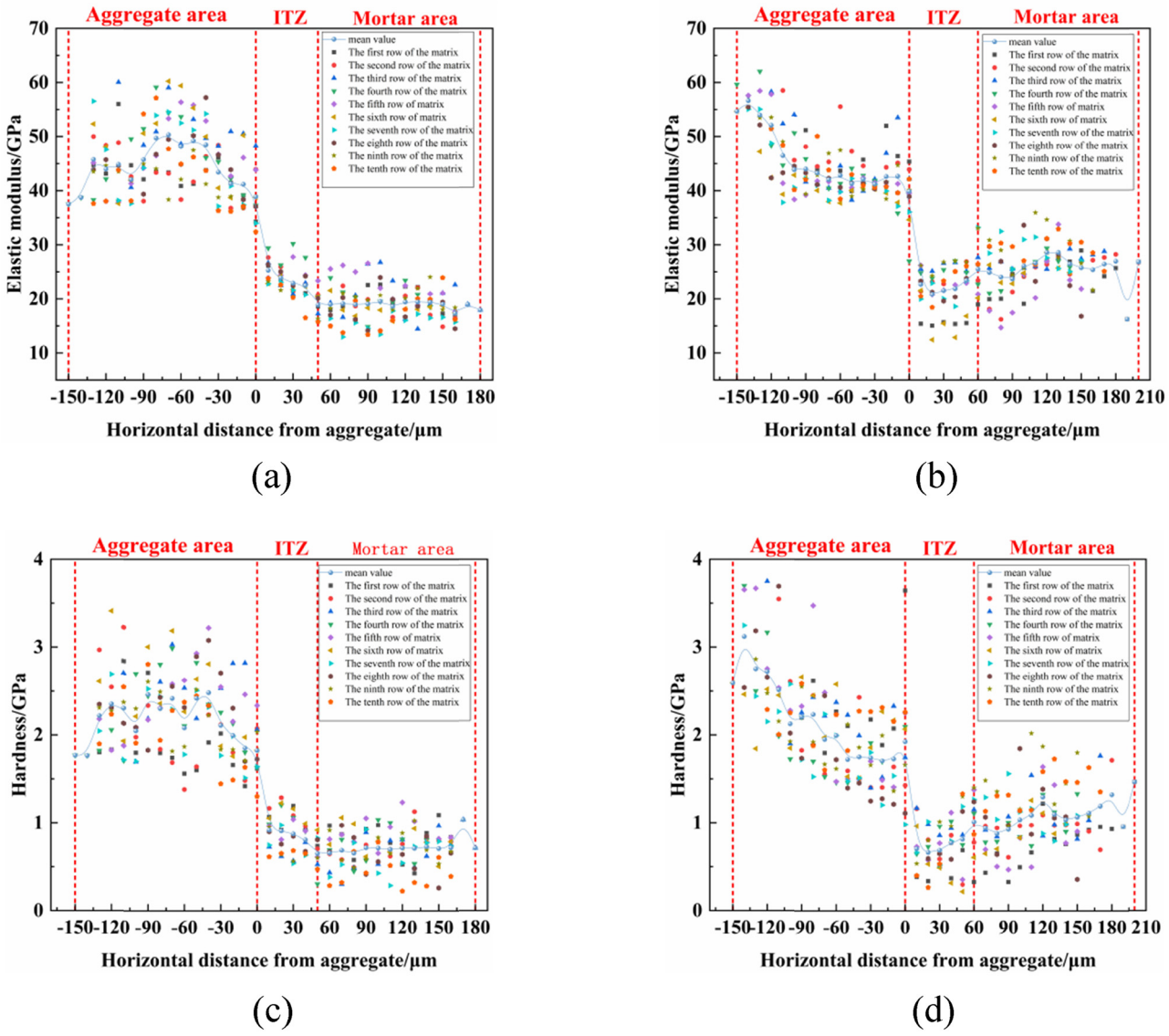

Figure 7: Graph of the distance between elastic modulus and hardness of different aggregate shapes and aggregate surface. (a) Elastic modulus at different distances from circular aggregate. (b) Elastic modulus at different distances from polygonal aggregate. (c) Hardness at different distances from round aggregate. (d) Hardness at different distances from polygonal aggregate.

and hardness show a decreasing then increasing and finally leveling off trend. When the distance from the surface of the polygonal aggregate is about 0–20 μm, the elastic modulus and hardness drop sharply and reach the minimum at about 20 μm. When the distance from polygonal aggregate surface is about 20–60 μm, the elastic modulus and hardness begin to increase. The micromechanical parameters tend to be relatively constant in the range of 60–200 μm from the surface of polygonal aggregate.

Zheng *et al.* [28] established a model of ITZ thickness and cement volume density using stereology method, and obtained that ITZ thickness of ordinary concrete is 20–56 μm. Chen *et al.* [29] quantitatively calculated the ITZ of cement composites with the help of the proximity function formula, and obtained that the thickness of the ITZ was less than 100 μm. According to the meso-zoning of concrete in Figures 7 and 8, the specimen is divided into three phases: aggregate, clean pulp, and ITZ. As can be seen from the figure, the interfacial zone of circular aggregate is relatively insignificant, about 50 μm around aggregate, while the interfacial zone of polygonal aggregate is about 60 μm around aggregate. The above micro-mechanical property data of aggregate regions with different shapes were statistically calculated, and the micromechanical property frequency curve of each phase and the table of mechanical properties of each phase were drawn, as shown in Figure 9 and Table 2.

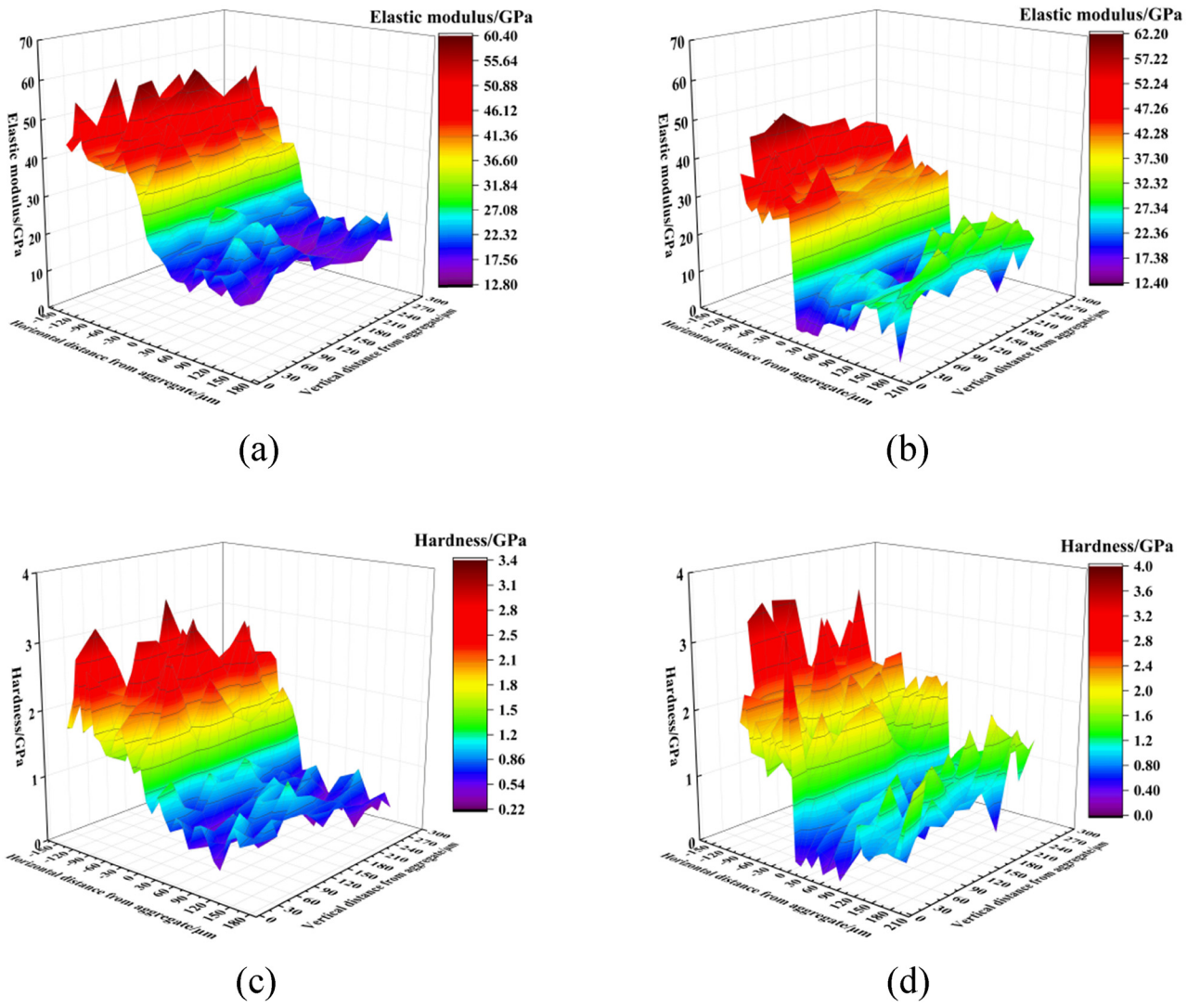

Figure 8: Cloud map of the distance between elastic modulus and hardness of different aggregate shapes and aggregate surface. (a) The change in elastic modulus of circular aggregate specimen. (b) The variation in elastic modulus of polygonal aggregate specimen. (c) Cloud diagram of hardness variation of round aggregate specimen. (d) Cloud diagram of hardness variation of polygonal aggregate specimen.

It can be seen from Figure 9 and Table 2 that the frequency distributions of elastic modulus and hardness between the interface of the specimen of circular aggregate and that of the specimen of clean aggregate are concentrated, with a small degree of dispersion, while the frequency distributions of elastic modulus and hardness between the interface of the specimen of polygonal aggregate and that of the pure paste are relatively dispersed, with a large degree of dispersion. By Gaussian fitting, the locations of the elastic modulus and hardness peaks of the aggregate, clean pulp, and ITZ of the circular aggregate specimen are (45.19 GPa, 2.19 GPa), (18.99 GPa, 0.7 GPa), and (23.65 GPa, 0.9 GPa), respectively. However, the locations of the elastic modulus and hardness peaks in the aggregate, clean pulp, and ITZ of polygonal aggregate specimens are (44.33 GPa, 2.1 GPa), (25.93 GPa, 1.06 GPa), and (21.66 GPa, 0.73 GPa), respectively.

The above results show that the elastic modulus and hardness of the interfacial phase of the circular aggregate specimen are slightly greater than the elastic modulus and hardness of the interfacial phase of the polygon aggregate specimen, and the interface area is relatively uniform. In contrast, the interfacial phase parameters around the polygon aggregate are uneven due to aggregate characteristics, and the interface area is relatively obvious, indicating that the micromechanical parameters of the interfacial phase of the circular aggregate are better. Existing research work has shown [30,31] that the larger the volume fraction of coarse aggregate, the more significant the effect of coarse

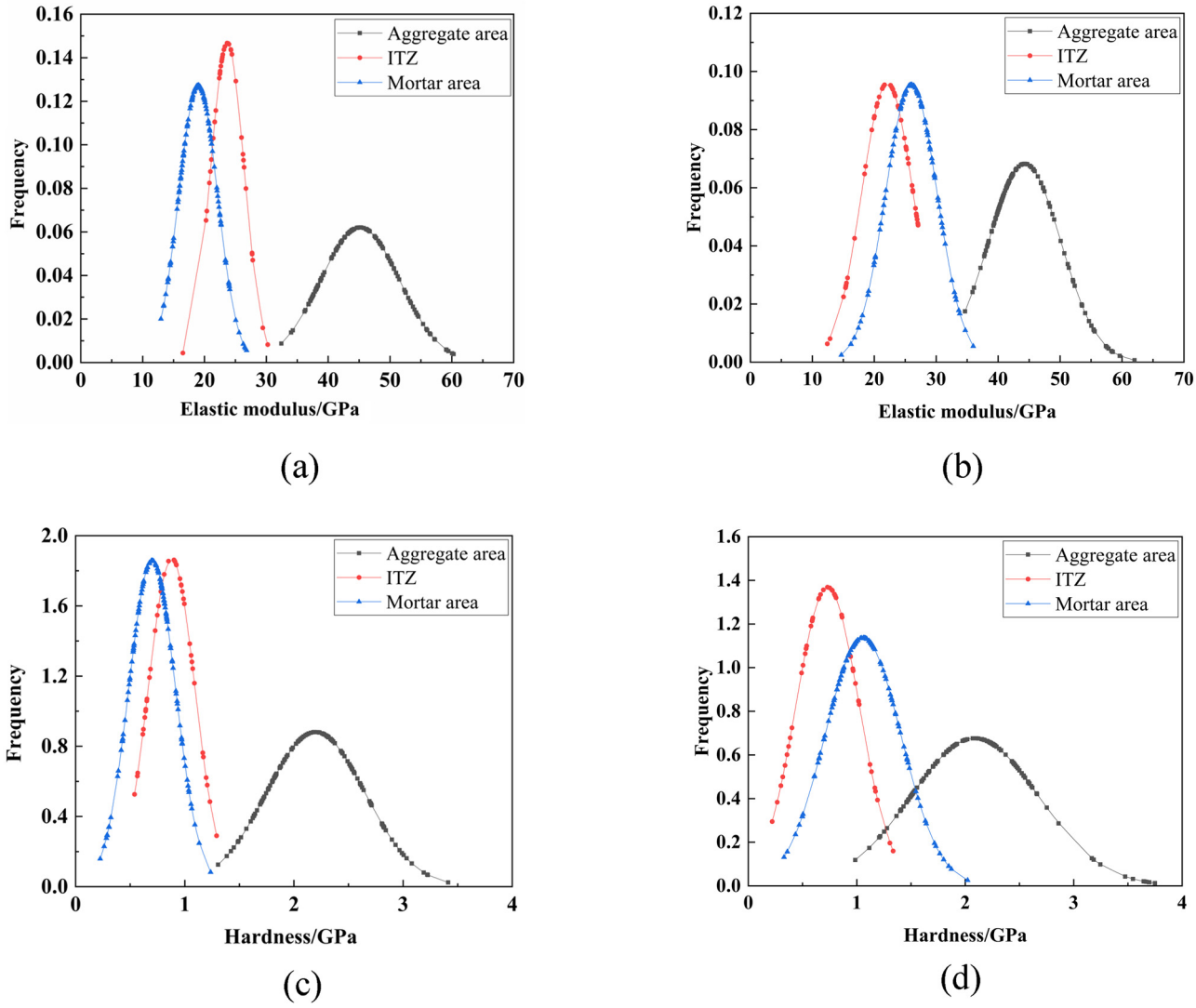

Figure 9: Frequency curves of nanomechanical properties of each phase with different aggregate shapes. (a) Frequency curve of elastic modulus of each phase of circular aggregate specimen. (b) Frequency curves of elastic modulus of each phase of polygonal aggregate specimen. (c) Hardness frequency curve of each phase of circular aggregate specimen. (d) Hardness frequency curve of polygonal aggregate specimen.

Table 2: Mechanical properties of each phase based on nanoindentation test

Aggregate shape	Nanomechanical properties	Aggregate		Clean pulp		Interfacial transition region	
		μ	σ	μ	σ	μ	σ
Circle	E/GPa	45.16	6.43	18.98	3.13	23.71	2.72
	H/GPa	2.2	0.45	0.7	0.21	0.88	0.21
Polygon	E/GPa	44.29	5.85	25.99	4.18	22.11	4.16
	H/GPa	2.08	0.59	1.06	0.35	0.73	0.29

aggregate shape on the modulus of elasticity, jade strength and compressive strength of concrete, and that spherical and ortho-polyhedral aggregates are more conducive to the improvement of the mechanical properties of concrete Irregularly shaped aggregates are more likely to produce more crystalline cracks than round aggregates.

The characteristic values of elastic modulus and hardness of each phase of the specimen processed by

Table 3: Microscopic parameters

Aggregate shape	Nanomechanical properties	Aggregate	Clean pulp	Interfacial transition region
Circle	E/GPa	45.19	18.99	23.65
	H/GPa	2.19	0.70	0.90
Polygon	E/GPa	44.33	25.93	21.66
	H/GPa	2.10	1.06	0.73

deconvolution analysis are shown in the following Table 3. The convolution data in the table are consistent with the nanomechanical properties of each material phase in the microstructure of the literature [32], which side by side proves the reasonableness of the interfacial zoning in this paper.

4.2 Influence of aggregate morphology on interfacial phase

In order to further compare the influence of aggregate properties on the interface, 1,000-fold electron microscope scanning was performed on the interfacial region of different aggregates.

It can be observed from Figure 10 that, at the hydration age of 7 days, the micro-surface morphologies of specimens with two different aggregate shapes are basically similar, and obvious hexagonal lamellar CH crystals and flocculent C–S–H gels are formed on the surfaces, so the aggregate shape has no significant influence on the generation of hydration products in the transition zone of the interface of specimens. Meanwhile, based on the results of nano-indentation test above, it can be seen that the elastic modulus and hardness of the ITZ of natural circular aggregate specimen are slightly higher than those of polygonal aggregate specimen, which is caused by the geometric characteristics of aggregate itself, and has nothing to do with physical and chemical factors.

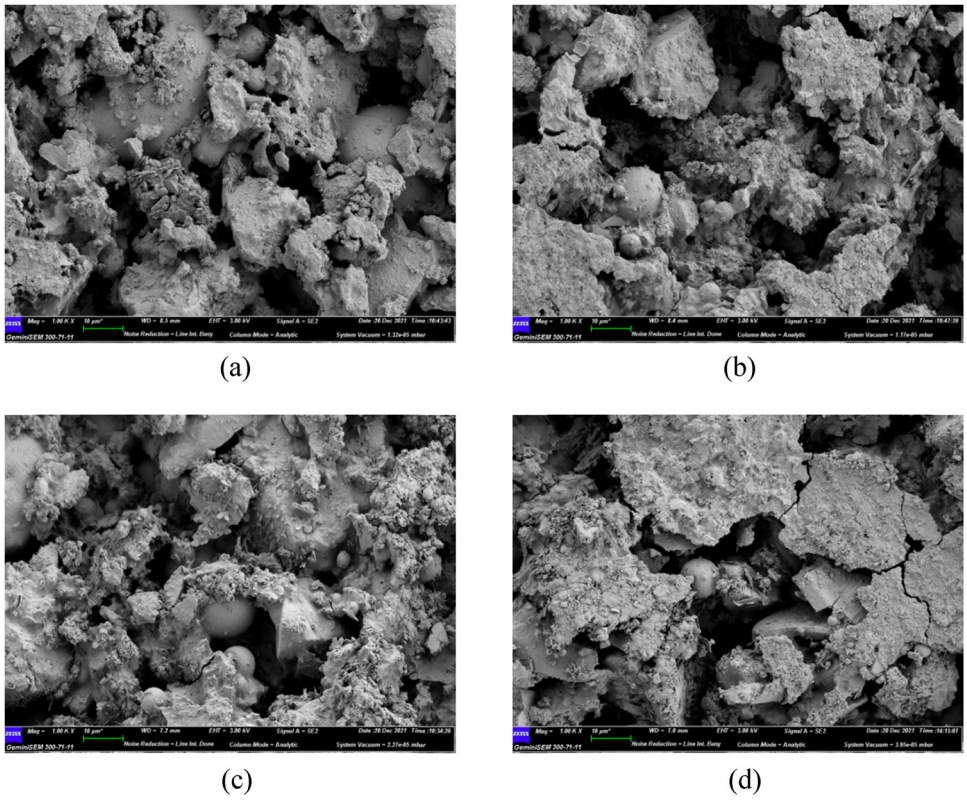

Figure 10: SEM images of the interface of aggregates with different shapes. (a) Circular aggregate interface SEM-1. (b) Circular aggregate interface SEM-2. (c) Polygonal aggregate interface SEM-1. (d) Polygonal aggregate interface SEM-2.

5 Conclusion

In order to explore the influence of different aggregate shapes on the interface region, this work uses nanoindentation and electron microscopy scanning to carry out micromechanical properties and phase tests on aggregate specimens of different shapes, and quantifies the width of the interface area and micromechanical parameters, analyzes the influence of aggregate shape on the interface area, and reveals the influence mechanism of aggregate shape on the interface region from the microscopic perspective, and the main conclusions are as follows:

1) Through the nanoindentation test, the interface area of the round aggregate specimen and the interface area of the polygon aggregate specimen were visually divided, and the width of the circular aggregate interface area was about 50 μm from the aggregate surface, while the width of the polygon aggregate interface area was about 60 μm from the aggregate surface, which was slightly larger than the circular aggregate interface area, indicating that the aggregate shape had a certain influence on the formation of the interface area width.
2) Gaussian fitting was performed on the microscopic experimental results to obtain micromechanical parameters. The analysis showed that the elastic modulus and hardness of the interface area of the circular aggregate specimen were better than those in the interface area of the polygon aggregate specimen, indicating that the circular aggregate had a positive effect on the formation of the interface area, and the micromechanical properties of the interface area were better.
3) Through the phase analysis of SEM test, it was observed that obvious hexagonal sheet layered CH crystals and flocculent C–S–H gels were formed at different aggregate shape interfaces, indicating that aggregate shape had no significant effect on the hydration products in the transition zone of the specimen interface. Therefore, the difference in the width of the interface area and micromechanical parameters of specimens of different aggregate shapes is mainly determined by the geometric characteristics of the aggregate itself. It provides reference significance for the development of microscopic theory of gelling sand gravel.

Funding information: This study was funded by National Natural Science Foundation of China (52109154); The Natural Science Foundation of Henan Province (202300410270); and Guiding River to assist Huai River (Henan section) engineering scientific research service project.

Author contributions: All authors have accepted responsibility for the entire content of this manuscript and consented to its submission to the journal, reviewed all the results and approved the final version of the manuscript. ZJ: methodology and writing – original draft. LG: supervision, methodology, and writing – review and editing. LZ: conceptualization and investigation. YY: data acquisition and writing – review and editing.

Conflict of interest: Authors state no conflict of interest.

Data availability statement: All data, models, and code generated or used during the study are available in the published article.

References

[1] Caijun S, Qiang Y. Test and analysis method of cement-based materials. 1, Beijing: China Architecture and Building Press; 2018.
[2] Alexander MG. Role of aggregates in hardened concrete, material science of concrete III. The American Ceramic Society, Inc; 1989. p. 119–46.
[3] Golewski GL. Concrete composites based on quaternary blended cements with a reduced width of initial microcracks. Appl Sci. 2023;13(12):7338.
[4] Golewski GL. The effect of the addition of coal fly ash (CFA) on the control of water movement within the structure of the concrete. Materials. 2023;16(15):5218.
[5] Golewski GL. Investigating the effect of using three pozzolans (including the nanoadditive) in combination on the formation and development of cracks in concretes using non-contact measurement method. Adv Nano Res. 2024;16(3):217.
[6] Huang X. Effect of coarse aggregate shape on physical and mechanical properties of concrete. Hangzhou: Zhejiang University of Technology; 2010 (in Chinese).
[7] Basheer L, Basheer PAM, Long AE. Influence of coarse aggregate on the permeation, durability and the microstructure characteristics of ordinary Portland cement concrete. Constr Build Mater. 2005;19(9):682–90.
[8] Kaplan MF. The effects of the properties of coarse aggregates on the workability of concrete. Mag Concr Res. 1958;29(10):63–74.
[9] Shergold FA. The percentage voids in compacted gravel as a measure of its angularity. Mag Concr Res. 1953;13(5):3–10.
[10] Murdock LJ. The workability of concrete. Mag Concr Res. 1960;36(12):135–14.
[11] Shi Y, Yang H, Chen X, Li X, Zhou S. Effect of aggregate type on pore structure and micro-interface of concrete. J Build Mater. 2015;18(1):133–8.
[12] Yehia S, Abdelfatah A, Mansour D. Effect of aggregate type and specimen configuration on concrete compressive strength. Crystals. 2020;10(7):625.
[13] Wu KR, Chen B, Yao W. Effect of coarse aggregate type on mechanical properties of high-performance concrete. Cem Concr Res. 2001;31(10):1421–5.

[14] Velez K, Maximilien S, Damidot D. Determination by nanoindentation of elastic modulus and hardness of pure constituents of Portland cement clinker. Cem Concr Res. 2001;31(4):555–61.
[15] Constantinides G, Ulm FJ, Van Vliet K. On the use of nanoindentation for cementitious materials. Mater Struct. 2003;36(3):191–6.
[16] Constantinides G, Ulm FJ. The nanogranular nature of C–S–H. J Mech Phys Solids. 2007;55(1):64–90.
[17] Wu D. Study on elastic modulus of concrete based on Nano-indentation technology and homogenization theory. Shanghai: Shanghai Jiao Tong University. 2019.001744.
[18] Zhou W, Sun W, Chen C, Miao C. Characterization of micromechanical properties of cement-based materials by nano-indentation technique. J Southeast Univ (Nat Sci Ed). 2011;41(2):370–5 (in Chinese).
[19] Smerdova O, Pecora M, Gigliotti M. Cyclic indentation of polymers: Instantaneous elastic modulus from reloading, energy analysis, and cyclic creep. J Mater Res. 2019;34(21):3688–98.
[20] Wang P, Qiao H, Zhang Y. Meso-damage evolution analysis of magnesium oxychloride cement concrete based on X-CT and grey-level co-occurrence matrix. Constr Build Mater. 2020;255:119373.
[21] Yin Y, Ren Q, Shen L, Han Y. Study on crack propagation and damage evolution process of concrete based on fractal dimension. J Hydraul Eng. 2021;52(11):1270–80.
[22] Jiang J. Microstructure testing and nanoindentation characterization of cementitious materials. Shanghai: Shanghai Jiao Tong University; 2018.
[23] Vandammeb M, Ulm F-J. Nanoindentation analysis as a two-dimensional tool for mapping the mechanical properties of complex surfaces. J Mater Res. 2009;24(3):679–90.
[24] Bobji MS, Biswasa SK. Deconvolution of hardness from data obtained from nanoindentation of rough surfaces. J Mater Res. 1999;14(6):2259–68.
[25] Li W, Xiao J, Huang L, Hah SP. Experimental study on nanomechanical properties of Regenerated concrete interfacial transition zone. J Hunan Univ (Nat Sci Ed). 2014;41(12):31–9.
[26] Li Y, Guan X, Liu S, He H, Wei H. Influence of indentation number and deconvolution method on nano-indentation test of cement. J Build Mater. 2021;24(2):291–5 + 312.
[27] Oliver WC, Pharr GM. An improved technique for determining hardness and elastic modulus using load and displacement sensing indentation experiments. J Mater Res. 1992;7(6):1564–83.
[28] Zheng JJ, Li CQ, Zhou XZ. Characterization of microstructure of interfacial transition zone in concrete. ACI Mater J. 2005;102(4):265.
[29] Chen HS, Sun W, Stroeven P. Quantitative solution of volume fraction of interface in cementitious composites. Acta Mater Compos Sin. 2006;23(2):133 (in Chinese).
[30] Tasdemir MA, Karihaloo BL. Effect of aggregate volume fraction on the fracture parameters of concrete: a meso-mechanical approach. Mag Concr Res. 2001;53(6):405–15.
[31] Jiang S, Shen L. Aggregate shape effect on fracture and breakage of cementitious granular materials. Int J Mech Sci. 2022;220:107161.
[32] Zhao S, Sun W. Application and research progress of nano-indentation in cement-based materials. J Chin Ceram Soc. 2011;39(1):164–76.